Educational simulations of spectral color dispersion in negative index prisms

Francisco L. Naranjo-Correa[(1)], Guadalupe Martínez-Borreguero[(1)]

(1) Department of Didactics of Experimental Sciences. Universidad de Extremadura (Spain)

Abstract:

Using a free, open-source ray-tracing program, photorealistic spectral images have been created to show how several prisms would appear in the real world if they were made with materials that have a negative index of refraction (metamaterials). The aim of this work is to provide students with a visual interpretation of the atypical behavior of negative-index materials and a look at dispersion in the visible range in such prisms, resulting in educationally valuable outcomes.

1. Introduction

Light dispersion through prisms is a fundamental phenomenon taught in physics curricula at various educational levels. Prisms made with conventional materials, such as glass, refract light based on their refractive index and geometry, resulting in a spectrum of colors. However, recent advancements in materials science have led to the development of negative-index materials, which exhibit unique properties and offer new opportunities for exploring light behavior. This study aims to provide an educational tool to enhance understanding of spectral color dispersion in negative-index prisms.

In an isotropic material, its refractive index (n) can be defined in terms of its electric permittivity (ε) and its magnetic permeability (μ) as:

$$n = \sqrt{\varepsilon \cdot \mu} \tag{1}$$

In general, ε and μ are complex numbers, with their imaginary parts responsible for the losses of the material, which can cause the absorption of electromagnetic radiation

passing through it. However, when losses are negligible, the imaginary parts of ε and μ are very small or close to zero, and the material is nearly transparent to electromagnetic radiation. To simplify the analysis, we will assume that the losses are negligible, and therefore ε and μ are treated as real parameters. As the typical transparent materials have positive ε and μ, the positive square root is used for n by convention, but it is evident that a simultaneous change in the sign of ε and μ has no effect whatsoever on the equation. In 1968, Veselago [1] inferred that the existence of materials with simultaneously negative electric permittivity and a negative magnetic permeability implied that the refractive index of such material would be negative. At that time, the proposal was only a thought experiment, but recent studies have shown the feasibility of engineering artificial materials with this property [2]–[12], usually known as metamaterials. Most of these metamaterials have been demonstrated at frequencies ranging from microwave to infrared, and recent results have been achieved in the visible region [13]–[17].

Several researchers pondered on what an isotropic material with a negative refractive index would look like at visible frequencies. They were curious about whether light passing through such materials would experience anomalous dispersion, which is a phenomenon where the refractive index decreases with an increasing wavelength. To investigate this question, photorealistic images of these materials were generated using POV-Ray [18], an open-source raytracer. The objective of these images was to provide scientists and laypersons with an intuitive and visual understanding of negative-index materials, whose surprising results would be pedagogically useful [19]–[22]. Moreover, POV-Ray has been extensively employed to teach optics and color [22]–[25].

2. Objectives

The goal of this paper is to build upon previous works, focusing on the educational aspect of the phenomenon of chromatic dispersion. To achieve this goal, a tool has been developed to generate spectral renderings of photorealistic images depicting how light behaves when passing through simple optical devices such as lenses, prisms, and flat-parallel plates. The aim of this educational tool is to provide students with an intuitive and visual understanding of the phenomenon of spectral color dispersion, both in positive and negative index prisms. By contrasting the classical dispersion phenomenon with negative index dispersion, students can develop a better understanding of the former.

The target audience includes high school students, undergraduate students, and pre-service science teachers who should possess a basic understanding of optics and electromagnetism, including the concepts of refraction, diffraction, and dispersion. Additionally, they should understand basic principles of optics, such as the behavior of light when passing through lenses, prisms, and flat-parallel plates. The tool can be used in the final years of high school, as well as in courses such as introductory optics, physical optics, or electromagnetism at the university level, and in pre-service science teacher courses.

The tool presented in this paper will enable teachers to provide their students with a deeper understanding of chromatic dispersion. The expected educational outcome for teachers who use this tool is that their students will be able to understand the physical

principles underlying the dispersion of light in negative index prisms and how it differs from traditional positive index prisms. By using negative index prisms, students will be able to compare the behavior of light in classical dispersion with that in negative index dispersion, which will enable them to better understand the former phenomenon. The tool will also enable students to explore and visualize the behavior of light in different scenarios and geometries, such as varying angles of incidence or thickness of the prism. This will help students develop their critical thinking and problem-solving skills, as well as gain a deeper understanding of the physics behind color dispersion and its potential applications in optics and other fields.

3. Method

3.1. Spectral rendering with POV-Ray

As noted above, previous studies [19]–[21] have validated the use of the POV-Ray raytracer to render photorealistic images of materials with negative index of refraction. However, there is one inconvenience with POV-Ray; internally, it does not perform spectral calculations. Instead of computing and storing light intensities for every wavelength, POV-Ray uses an additive representation of color with only three values (red, green, and blue or RGB), which saves computing time and memory. However, this method introduces color distortion and produces physically incorrect images [26]. This is a significant disadvantage when working with simulations involving dispersion phenomena since the program is unable to perform them due to considering the refractive index constant for all wavelengths.

All materials, however, have unique spectral responses; thus, to provide fully correct colorimetric results, all calculations should be done wavelength by wavelength. To achieve this, a member of the POV-Ray developer community [27] implemented this idea in the program, so that it could be used as a spectral rendering engine. This method works by rendering a set of grayscale images, each representing a specific wavelength. The output is a collection of thirty-six high dynamic-range [28] images that correspond to the wavelengths ranging from 380 to 730 nm in 10 nm increments. Finally, the thirty-six images are combined and converted to tristimulus values using the CIE color matching function in the last step of the calculation. To illustrate how spectral rendering works in POV-Ray, Figure 1 shows, by way of example, the dispersion of a beam of light (CIE D65 illuminant) when passing through a prism.

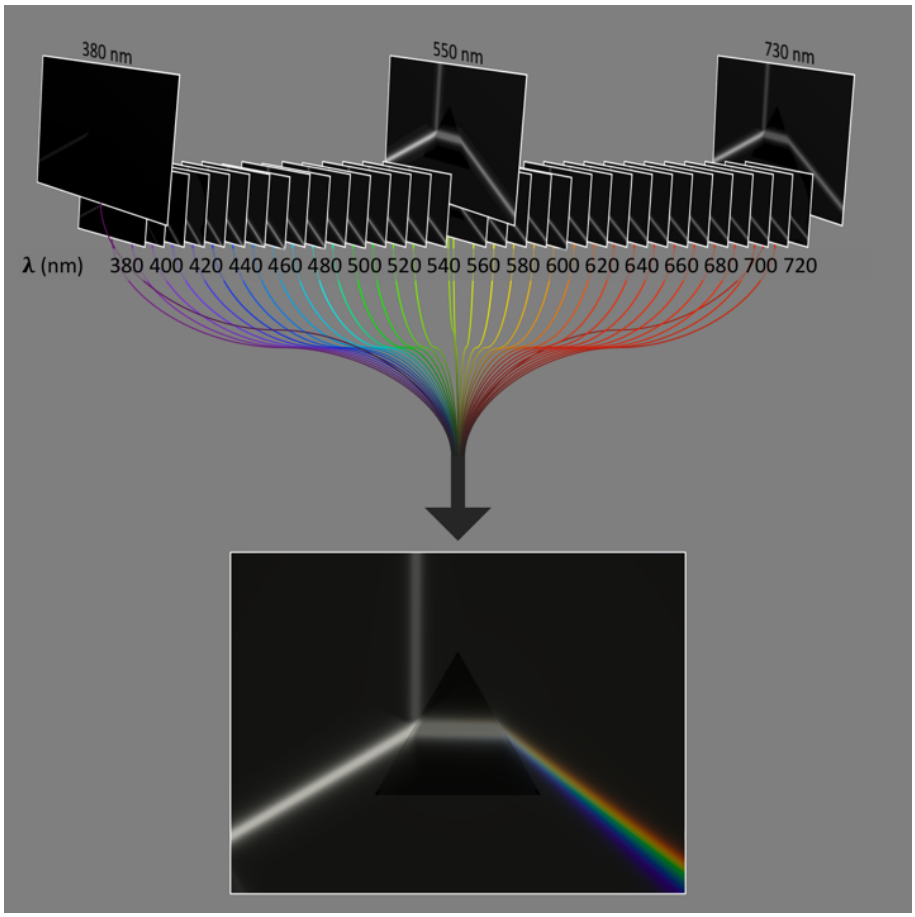

Figure 1. Spectral rendering in POV-Ray. The rendered set of grayscale images, each representing a specific wavelength (from 380 nm to 730 nm in steps of 10 nm), is combined in the final composite image using the CIE color matching function.

3.2. Defining variable indexes of refraction in POV-Ray

The refractive indexes in POV-Ray spectral rendering are calculated using the Sellmeier equation [29]:

$$n^2(\lambda) = 1 + \frac{B_1\lambda^2}{\lambda^2 - C_1} + \frac{B_2\lambda^2}{\lambda^2 - C_2} + \frac{B_3\lambda^2}{\lambda^2 - C_3} \tag{2}$$

Where B_i and C_i are the Sellmeier coefficients (experimentally determined). As an example, the coefficients for the Schott's N-SF11 flint glass used in the prism in Figure 1, obtained from online databases [30], [31], are shown in Table 1:

Table 1. Sellmeier coefficients of N-SF11 flint glass

B_1	B_2	B_3	C_1	C_2	C_3
1.73759695	0.313747346	1.89878101	0.013188707 μm²	0.0623068142 μm²	155.23629 μm²

To determine *n* from Eq. 2, we must calculate the square root of the right-hand side. Normally, the positive root is used to obtain the conventional index of refraction but, in our case, we also use the negative root to define the refractive index of simulated metamaterials. Thus, we can obtain the corresponding metamaterial of each real material in terms of n. For instance, by using the values in Table 1 we can obtain the negative index of refraction of a Schott's N-SF11 "metaglass" (denoted N-SF11-M). In practical terms, we can say that the refractive index of our simulated metamaterials is obtained by multiplying the value of the refractive index of its real counterpart by -1.

3.3. Educational aspects

As stated in the Objectives section, the tool is intended for high school students, undergraduate students, and pre-service science teachers. The tool can be effectively utilized in various educational settings, including the final years of high school, as well as in courses such as introductory optics, physical optics, or electromagnetism at the university level, and in pre-service science teacher courses.

In the context of high school education, the tool can be incorporated into the final years of high school physics courses. For example, during a unit on optics, students can explore the dispersion characteristics exhibited by regular (positive index) and negative index materials using the provided images. They can compare and discuss the differences in how light interacts and propagates through these materials, examining topics such as the bending of light, color dispersion, and the unique optical properties of negative index materials. This hands-on exploration allows students to deepen their understanding of fundamental concepts in optics and gain insight into cutting-edge materials research.

At the undergraduate level, the tool can be integrated into courses such as introductory optics, physical optics, or electromagnetism. In these courses, students can delve deeper into the principles of light propagation and dispersion. They can use the generated images and simulations as visual aids to analyze and interpret the behavior of light in both positive and negative index materials. This interactive approach fosters active learning, allowing students to explore advanced topics and develop a deeper appreciation for the complexity of light-matter interactions.

Pre-service science teacher courses also provide an ideal setting for incorporating the educational tool. Future science teachers can use the tool to enhance their pedagogical knowledge and instructional practices in optics. They can explore different teaching strategies and activities that utilize the images and simulations to engage students in discussions and hands-on experiments. By incorporating the tool into their teaching repertoire, pre-service science teachers can inspire their future students to explore the field of optics and stimulate their curiosity in materials science.

To facilitate a comprehensive understanding of the behavior of light in different materials, students are encouraged to compare and discuss the dispersion characteristics exhibited by regular (positive index) and negative index materials. By contrasting these two types of materials, students can explore the fundamental differences in the way light interacts and propagates through them. Through the examination and analysis of the dispersion

characteristics of both positive and negative index materials, students can gain valuable insights into the unique optical properties and applications of negative index materials.

Engaging in a comparative discussion of dispersion in regular and negative index materials opens opportunities to delve into the underlying principles and mechanisms that govern light propagation. By exploring these topics, students can develop a deeper understanding of how different materials interact with light and how dispersion phenomena play a crucial role in various optical applications. This analytical approach fosters critical thinking skills and encourages students to delve into the intricacies of light behavior, ultimately fostering a broader appreciation for the diverse properties of materials in the context of optics and photonics.

In conclusion, the utilization of this educational tool in high school, undergraduate, and pre-service science teacher settings offers several valuable educational outcomes. For students, it fosters a comprehensive understanding of light behavior in different materials, allowing them to analyze and interpret dispersion phenomena and apply their knowledge to real-world optical applications. Engaging in comparative discussions and analytical thinking promotes critical thinking skills and a deeper appreciation for the diverse properties of materials in the context of optics and photonics. For pre-service science teachers, incorporating this tool enhances their pedagogical knowledge and instructional practices in optics, equipping them with effective techniques and resources to inspire future students to explore the field of optics and stimulate their curiosity in materials science. Ultimately, the use of this tool promotes active learning, critical thinking, and deeper comprehension of optical concepts, benefiting both students and teachers in their educational journey.

4. Results

As stated before, the primary outcome of this work is the generation of photorealistic images of negative index prisms, which serve as valuable visual aids for educational purposes. These images capture the behavior of light in interaction with negative index materials and demonstrate the spectral color dispersion phenomena that occur. By showcasing the unique properties of negative index prisms, these images provide a clear and engaging representation of light propagation in these materials.

To make the generated images easily accessible to teachers and students, they are provided as digital supplementary material [32]. This ensures that educators can incorporate them into their teaching materials and students can directly engage with the visual representations while studying the concepts of light dispersion and refraction. The POV-Ray code is available upon request.

Figure 2 shows some of the simulated prisms used in this work. The left side of the image depicts normal prisms with refractive index greater than 1, while the right side shows metaprisms with refractive index less than -1.

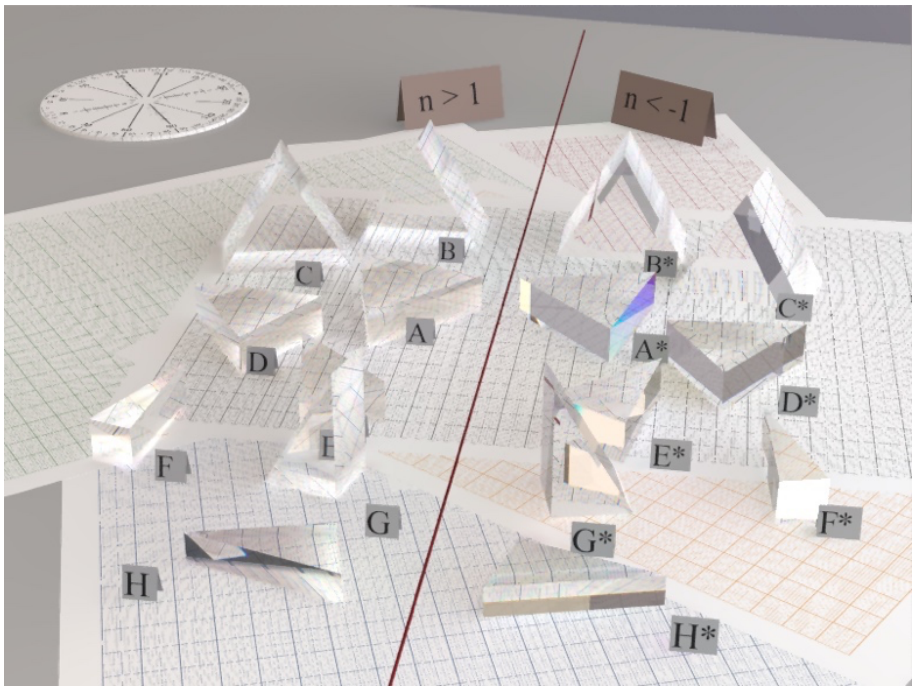

Figure 2. Simulated prisms (left) and metaprisms (right).

The prisms used in this study are labeled as follows, with an asterisk denoting those with negative refractive index (metaprisms): (A) N-SF11 dense flint glass prism, α = 60°; (B) F2 flint glass prism, α = 60°; (C) K7 crown glass prism, α = 60°; (D) N-SF11 dense flint glass prism, α = 45°; (E) N-SF11 dense flint glass prism, α = 30°; (F) N-SF11 dense flint glass prism, α = 15°; (G) N-SF11 dense flint glass Abbe prism; (H) N-SF11 dense flint glass Littrow prism.

In the following sections we will discuss how a beam of white light (CIE Standard Illuminant D65 [33]) is dispersed by each of these prisms.

4.1. Equilateral prisms

In the example shown in Figure 1, we see the typical case of dispersion in an equilateral N-SF11 prism with an angle of incidence $\theta_1 = 60^{\circ}$. If we replace the prism with a metaprism made of N-SF11-M glass, we obtain the result displayed in Figure 3.

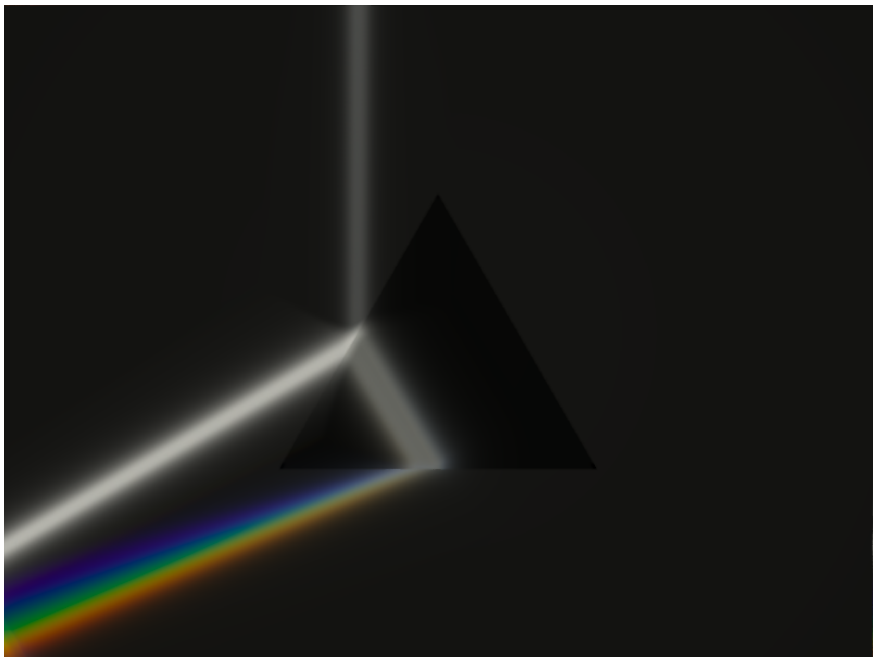

Figure 3. A beam of white light dispersed by an equilateral metaprism.

The most remarkable feature is the significant deflection of the emerging beam. Unlike in conventional materials where the light passes through the prism, in this case, the light beam refracts in a way that dramatically alters its direction, eventually emerging from the base. Figure 4 shows a detailed depiction of the trajectory of the rays.

Figure 4 (top) depicts the ray diagram of a light beam with an angle of incidence $\theta_1 = 60^o$, impinging on the AB side of an equilateral prism ($\alpha = 60^o$) made of dense N-SF11 flint glass (chosen for its high dispersive nature). In the middle part of the figure, the glass is replaced with a N-SF11-M type metaglass, while maintaining the angle of incidence ($\theta_1 = 60^o$). It can be observed that the beam is refracted towards the "wrong" side of the normal. In the metaprism, the angle θ_2 is the same as in the prism, but it deviates towards the opposite side of the normal, causing the beam to emerge from the base (BC) instead of the opposite side (AC)). At the base, the beam undergoes another refraction, emerging with an angle θ_4, which has the same value but opposite sign as its real counterpart.

As the beam emerges from the base, the top angle α is not involved in the refraction of the metaprism. If we wish for the beam to reach the AC side and "pass through" the prism in the conventional way, we must alter the angle of incidence θ_1 to change its sign and make it impinge from the opposite side of the normal. As shown in Figure 4 (bottom), by changing the angle of incidence from one side of the normal to the other, the beam can effectively pass through the prism and emerge from the AC side, with the angle α once again playing a role in the refraction.

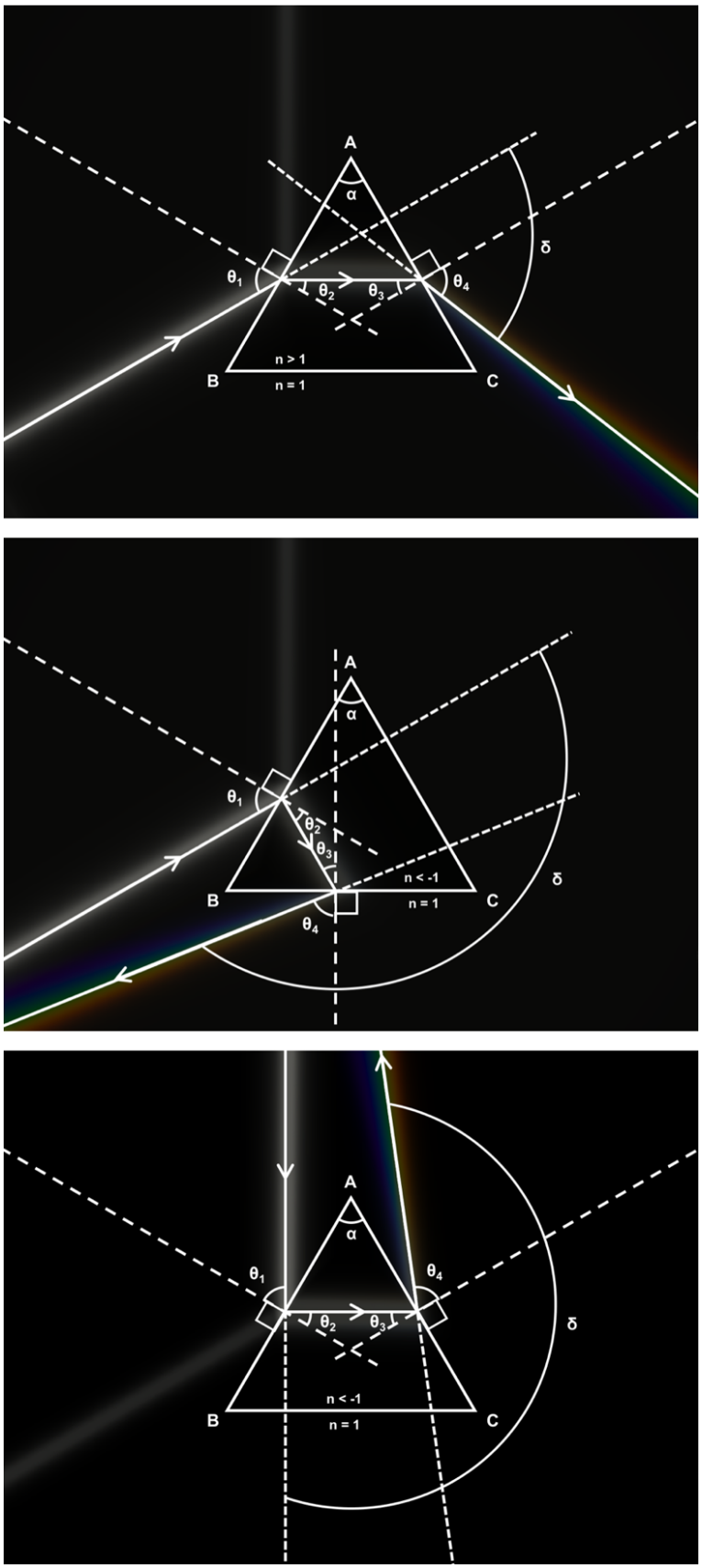

Figure 4. Diagram of rays in equilateral prisms. Top: N-SF11 glass, $\theta_1 = 60º$. Middle: N-SF11-M metaglass, $\theta_1 = 60º$. Bottom: N-SF11-M metaglass, $\theta_1 = -60º$.

To calculate the emergence angle in the prism the following expression can be used:

$$\theta_4 = \arcsin\left(\sin\alpha\sqrt{n^2 - \sin^2\theta_1} - \cos\alpha\sin\theta_1\right) \quad (3)$$

In a metamaterial this expression is still valid, if the arcsine argument is between -1 and 1, which is possible if we take the negative sign of the root again. In the examples illustrated in Figure 4 we obtain, for λ = 580 nm, the results indicated in Table 2:

Table 2. Notable angles on the simulated prisms (λ = 580 nm)

Material	*n*	θ_1	θ_4	δ
N-SF11	1.7859	60º	66º 52' 7"	66º 52' 7"
N-SF11-M	-1.7859	-60º	-66º 52' 7"	-186º 52' 7"

The deviation angle δ is calculated as:

$$\delta = \theta_1 + \theta_4 - \alpha \quad (4)$$

From this we can easily deduce the relationship between the deviation in a normal prism and its metamaterial counterpart (δ_M):

$$\delta_M = -(\delta + 2\alpha) \quad (5)$$

If the dispersion is examined, it can be observed that the metaprism produces a dispersion analogous to that of a normal prism, except for the inversion of the exit angle. To illustrate this more clearly, Figure 5 shows a beam of light composed of two pure emissions of 480 nm and 640 nm impinging on a prism (top) and a metaprism (bottom) with an incidence angle of θ_1 = 60º. It can be seen that the beam is dispersed in its two pure components, with the only difference being the orientation of the emergence angle relative to the normal axis.

In the classic prism, the emergence angle for the blue beam (λ = 480 nm) is θ_{4B} = 70º 21' 49", whereas for the red beam (λ = 640 nm), the emergence angle is θ_{4R} = 65º 43' 29" (thus, the separation angle between the two beams is $\Delta\theta_4$ = 4º 38' 21"). The corresponding deviation angles are δ_B = 70º 21' 49" and δ_R = 65º 43' 29".

In the metaprism, on the other hand, the beams deviate to the opposite side of the normal. As a result, the emergence angle for the blue beam is θ_{4B} = -70º 21' 49", and θ_{4R} = -65º 43' 29" for the red beam. The separation angle between the two beams is therefore the same that in the prism, $\Delta\theta_4$ = 4º 38' 21". The deviation angles, however, change drastically, with values of δ_B = -190º 21' 49" and δ_R = -185º 43' 29", in accordance with Eq. 5.

For visible light, in most transparent materials the refractive index decreases with increasing wavelength (known as normal dispersion). If the refractive index increases

with increasing wavelength, the material exhibits anomalous dispersion. According to this definition, anomalous dispersion might have been expected in our metaprism. However, the way in which we have defined the refractive index of our metamaterials implies normal dispersion, just like in the classic material. In both cases, the shortest wavelength (blue light, 480 nm) is bent more strongly than the longest wavelength beam (red light, 640 nm).

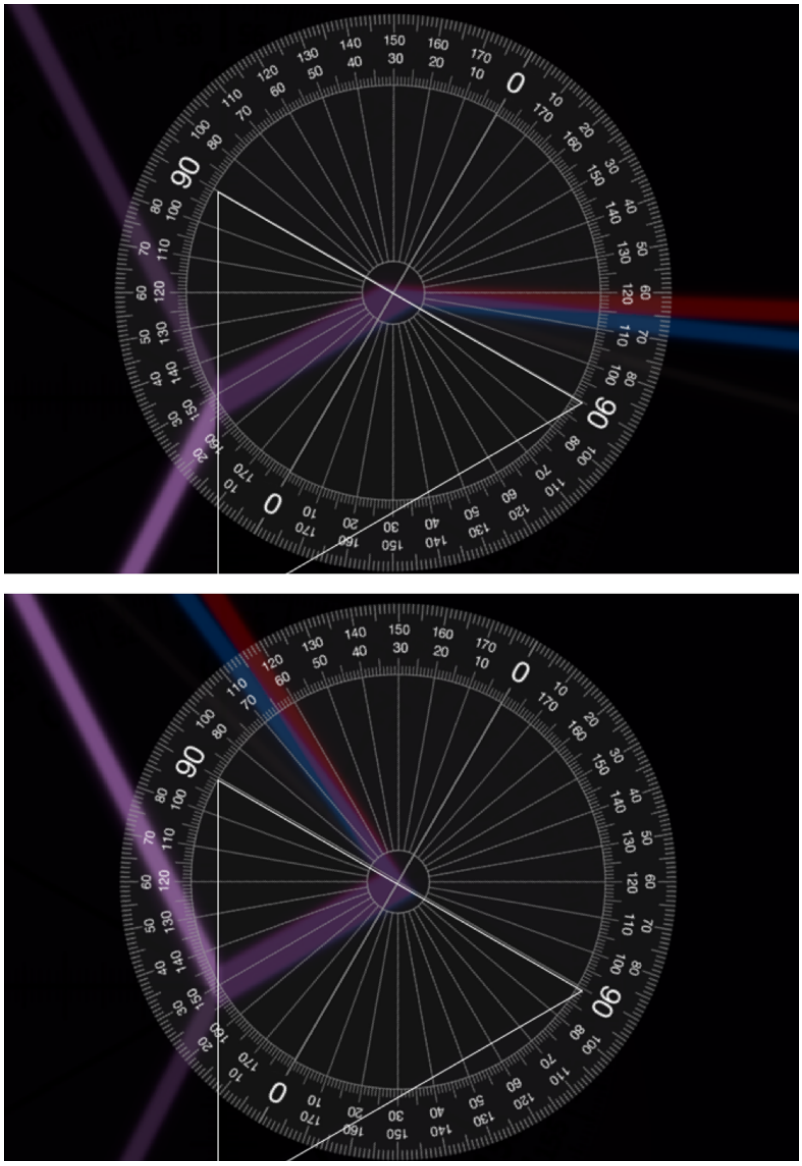

Figure 5. Dispersion of a 480 nm beam (blue) and a 640 nm beam (red) in a prism (top) and a metaprism (bottom).

Figure 6 illustrates how the angle of incidence affects the refraction of our prisms and metaprisms. In the left column, an equilateral N-SF11 flint glass prism is shown, where a beam of white light strikes at different angles of incidence, ranging from $\theta_1 = 15^\circ$ to $\theta_1 = 75^\circ$, at 15º intervals. It is observed that between $\theta_1 = 15^\circ$ and $\theta_1 = 45^\circ$ the beam undergoes total internal reflection on the AC side because it reaches it at an angle greater than the critical angle. For any $\theta_1 > 53^\circ\ 35'\ 58''$, a refracted beam is expected, as observed in the images for $\theta_1 = 60^\circ$ and $\theta_1 = 75^\circ$.

In the central column, an N-SF11-M metaprism is shown. If the same angles of incidence as in the prism are used, the beam inside the metaprism is refracted to the other side of the normal and directed to the base of the metaprism prism instead of the opposite side, as seen before. Like the real prism, the beam undergoes a total internal reflection, this time in the BC side (the base) between $\theta_1 = 15º$ and $\theta_1 = 45º$, until it is finally refracted in the base (images for $\theta_1 = 60º$ and $\theta_1 = 75º$).

Finally, the right-hand column depicts the same N-SF11-M metaprism as before, but with the angles of incidence reversed. It can be observed that the path of the beam inside the metaprism is exactly the same as the one followed in the real prism shown on the left column: there is a total internal reflection when $\theta_1 > -53º\ 35'\ 58''$, and the beam is dispersed on the AC side in $\theta_1 = -60º$ and $\theta_1 = -75º$.

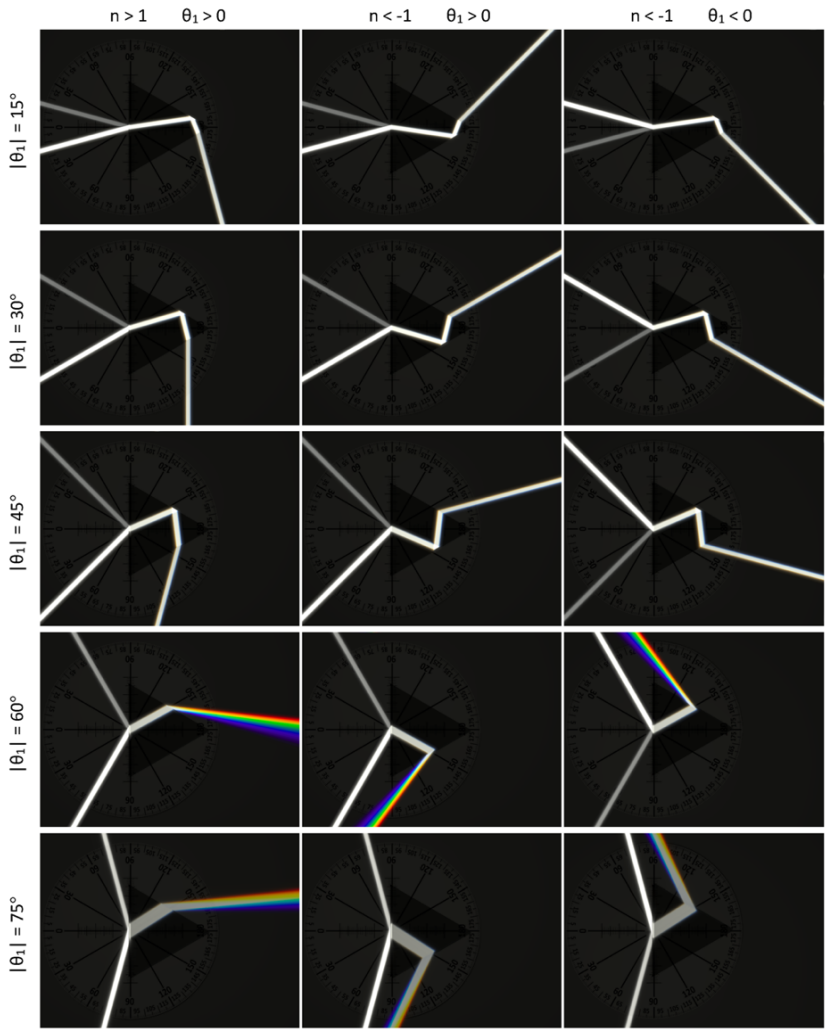

Figure 6. A white beam of light strikes at different angles of incidence on a prism (left column) and a metaprism (center and right columns). In the central column, the angle of incidence remains the same as in the left column, while in the right column the angle of incidence has the opposite sign.

As previously seen, one of the main factors that affect the behavior of dispersive prisms is their composition. In many applications, the prism is intended to have high dispersion, for which flint such as F2 or dense flint glasses like N-SF11 are used, while Crown glasses such as N-BK7 or K7 have a small dispersion for visible light.

The left column of Figure 7 shows these two types of prism: a highly dispersive prism made of F2 flint glass (top), and a low dispersion prism made of K7 crown glass (bottom). The right column of Figure 7 shows their metaprism counterparts. As expected, the flint prism, with large dispersive power, leads to large angular dispersion compared to the crown prism. By way of example, the deviation angles for $\lambda = 480$ nm and $\lambda = 640$ nm are shown in Table 3.

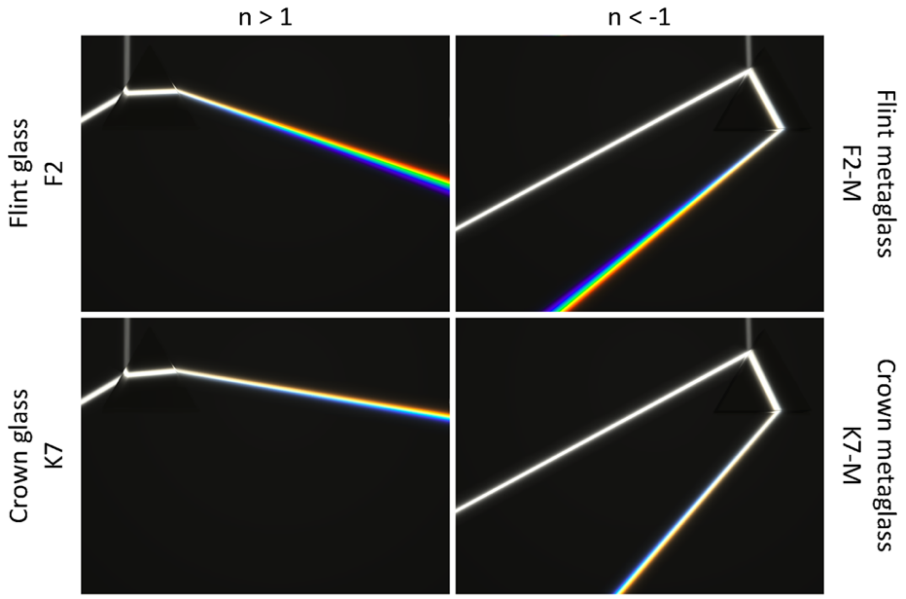

Figure 7. Highly dispersive (top) and low dispersive (bottom) prisms (left) and metaprisms (right).

Table 3. Deviation angles from Figure 7

	480 nm	640 nm	Δδ
Material	δ_{4B}	δ_{4R}	$\delta_{4B} - \delta_{4R}$
F2	50º 00' 03"	48º 28' 26"	1º 31' 37"
K7	40º 15' 09"	39º 35' 23"	0º 39' 46"
F2-M	-170º 00' 03"	-168º 28' 26"	-1º 31' 37"
K7-M	-160º 15' 09"	-159º 35' 23"	-0º 39' 46"

4.2. Isosceles prisms

Although equilateral prisms are often the most commonly used, the angle of the prism (α) can be selected to influence the exact dispersion characteristics required.

Dispersive prisms are usually used at the minimum deviation angle. This is the angle at which the wavelength of interest will travel parallel to the base of the prism, and the angle of incidence is equal to the angle of emergence when measured with respect to the normal of the respective prism face. The minimum deviation angle for a given wavelength can be calculated as:

$$\theta_1 = \arcsin\left(n \cdot \sin\frac{\alpha}{2}\right) \tag{6}$$

Figure 8 shows how the angle of the prism (the upper corner in the depicted prisms) affects dispersion in both our prisms and metaprisms. In the left column, there are 4 N-SF11 flint glass prisms, in which the angle of the prism is changed from α = 15º to α = 60º, at 15º intervals. A beam of white light strikes each of the prisms with its respective minimum deviation angle (calculated for λ = 580 nm). It can be observed that, in general, the path of the ray inside the prism runs parallel to the base, and how the dispersion increases as α (and, therefore, θ_1) increases.

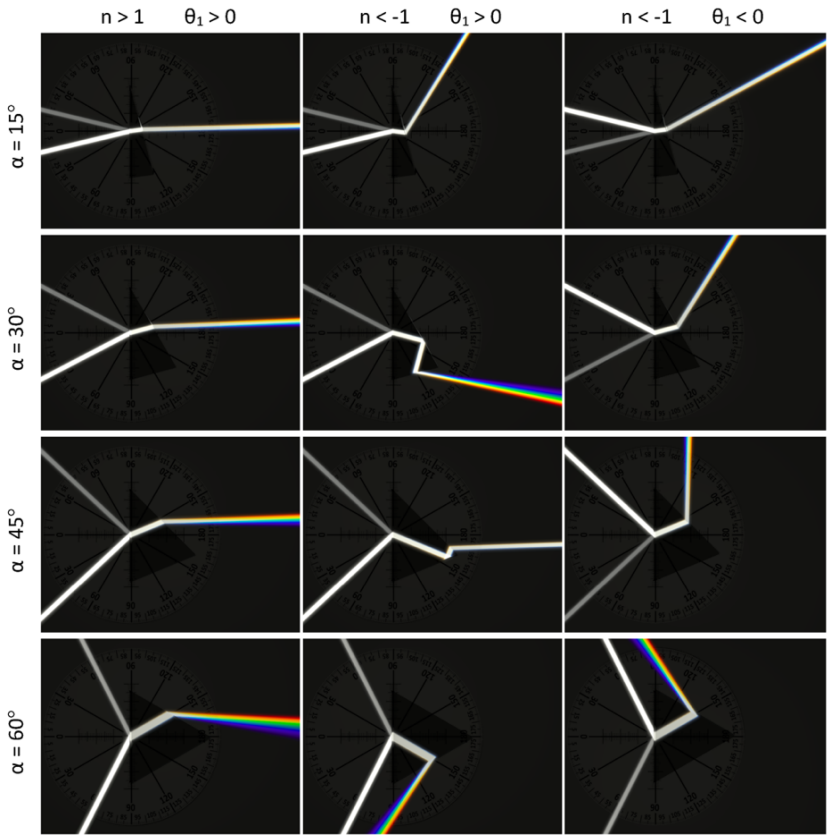

Figure 8. A white beam of light strikes on several prisms (left column) and metaprisms (center and right columns). The angles of incidence in the left and right columns are chosen to achieve minimum deviation. In the central column, the angle of incidence remains the same as in the left column.

In the central column, we have the N-SF11-M metaprism counterparts of the prisms. As expected, if the same angles of incidence as in the prism are used, the beam inside the metaprism is refracted to the other side of the normal, and consequently, it does not travel parallel to the base of the metaprism and exhibits an apparently erratic behavior. Notice how the beam only exits from the opposite side in the first case when $\alpha = 15^o$. When $\alpha = 30^o$, the beam suffers a total internal reflection on the AC side, so there is no refracted beam. In the remaining two cases, the beam emerges through the base, so the α angle does not influence the refraction and dispersion shown. To ensure that the beam travels parallel to the base, the angle of incidence must be reversed, as has been done on previous occasions. The right-hand column shows the same N-SF11-M metaprism as before, but with the angles of incidence reversed. As predicted, the path of the beam inside the metaprism is the same as the one followed in the real prism shown on the left column.

Table 4 shows the angles of incidence and deviation (calculated for $\lambda = 580$ nm) depicted in Figure 8.

Table 4. Incidence and deviation angles from Figure 8

	N-SF11		N-SF11-M		N-SF11-M	
α	θ_1	δ	θ_1	δ	θ_1	δ
15º	13º 28' 48"	11º 57' 36"	13º 28' 48"	-44º 37' 57"	-13º 28' 48"	-41º 57' 36"
30º	27º 31' 51"	25º 03' 42"	27º 31' 51"	n/a	-27º 31' 51"	-85º 03' 42"
45º	43º 06' 45"	41º 13' 31"	43º 06' 45"	n/a	-43º 06' 45"	-131º 13' 31"
60º	63º 14' 47"	66º 29' 33"	63º 14' 47"	n/a	-63º 14' 47"	-186º 29' 33"

4.3.Right-angle prisms

Figure 9 shows a N-SF11 prism (top) and a N-SF11-M metaprism (bottom) of 30º-60º-90º (also known as Abbe prism). Although these prisms are normally used to separate a single required wavelength from a light beam containing multiple wavelengths, in the arrangement of the figure, we have used them in such a way that the beam of white light is perpendicular to the hypotenuse ($\theta_1 = 0^o$; $\theta_2 = 0^o$). This way, the beam only suffers refraction when leaving the system, which allows for a more direct comparison of the differences in behavior between the prism and the metaprism.

In both cases, the angle of incidence when exiting the prism is $\theta_3 = 30^o$. For $\lambda = 580$ nm, $\theta_4 = 63^o\ 14'\ 47''$, in the prism and $\theta_4 = -63^o\ 14'\ 47''$ in the metaprism. Again, the blue light is bent more strongly than the red light.

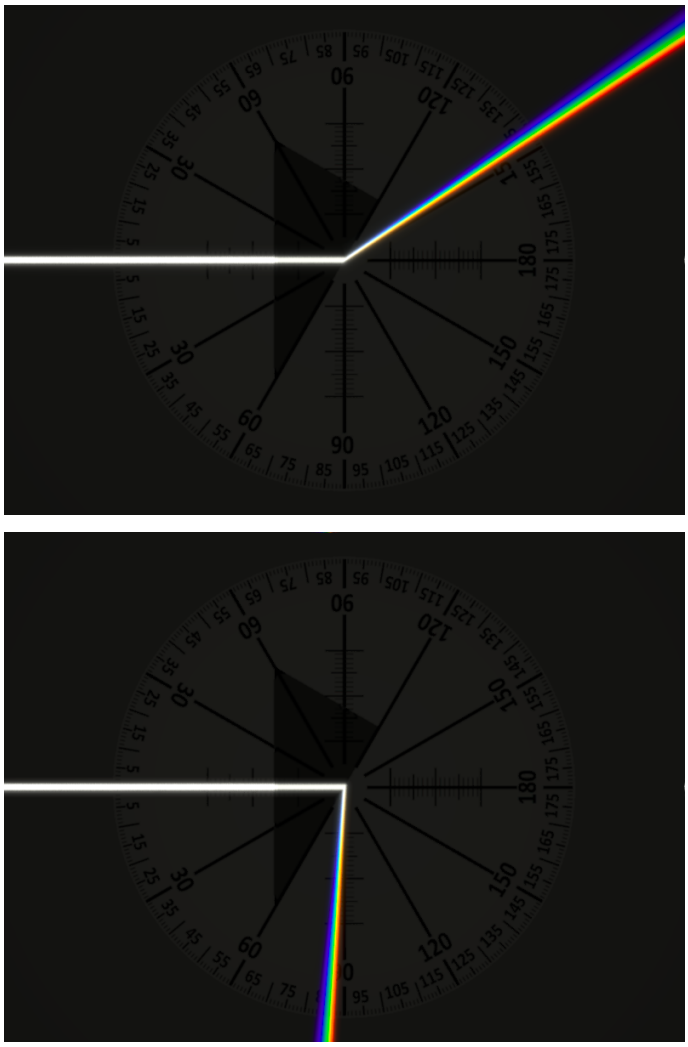

Figure 9. 30º-60º-90º prism (top) and metaprism (right) with a white beam impinging at $\theta_1 = 0º$.

Figure 10 depicts a N-SF11 Littrow prism (top left), a N-SF11-M Littrow metaprism (top right), a BK7 Littrow prism (bottom left) and a BK7-M Littrow metaprism (bottom right). Littrow prism are a retro-reflecting dispersing prism. In our simulations, they are based on the previous 30º-60º-90º prisms with a reflective coating on the surface opposite the 60° angle. Typically, Littrow prisms are used to separate a single required wavelength from a light beam containing multiple wavelengths by altering the angle of incidence. In our simulation, the angle of incidence is chosen to undergo minimal deviation, meaning the angle at which the light exits the prism is as close as possible to the angle at which it initially entered the prism. By inducing minimal deviation, the Littrow prism enables maximum dispersion of the incident light, which allows the different colors of light to be separated effectively. This maximum dispersion is desirable because it facilitates the analysis and identification of individual colors of light.

As expected, the flint prism and metaprism show higher dispersion than the crow prism and metaprism. Again, to obtain minimal deviation, the incidence angle in the metaprism must be inversed with respect to the normal axis of the incident face.

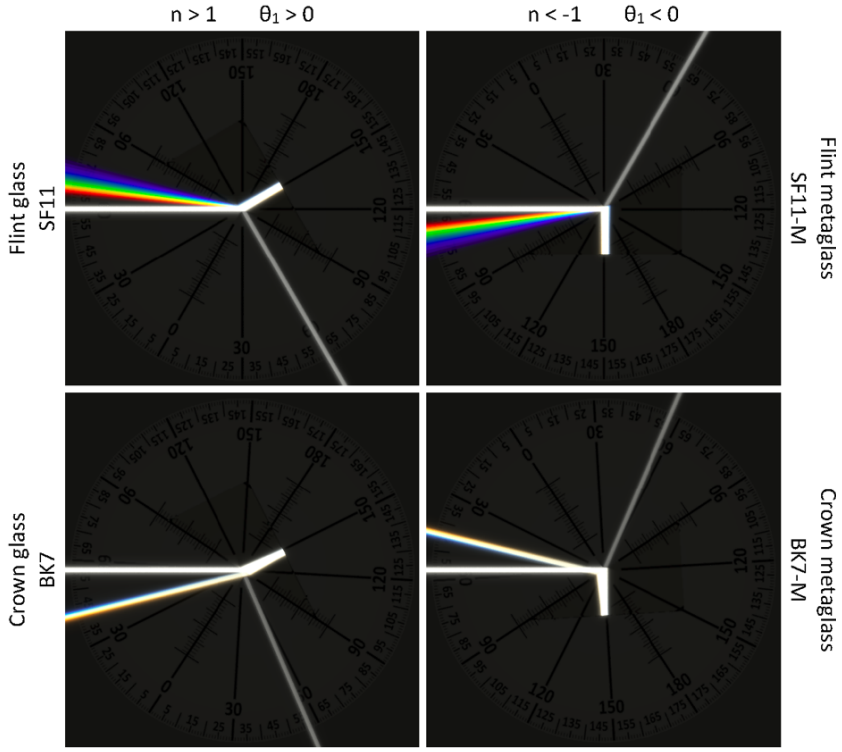

Figure 10. Littrow prisms (left) and metaprisms (right) made with different kind of glass, with a white beam impinging at the appropriate angle to obtain minimum deviation.

4.4.Prism pairs

Figure 11 depicts combinations of two equilateral N-SF11 prisms (top), one N-SF11 prism and one N-SF11-M metaprism (middle) and two metaprisms (bottom).

In the arrangement of the two prisms (Figure 11, top), we observe how the beam dispersed in the first prism enters the second one and then exits as a spectrum where the different wavelengths emerge in parallel, in the same direction as the original white beam. The empty space between the two prisms results in the beam separating into its spectral components and not recombining into a white light beam, as is wrongly indicated in many textbooks.

If we replace the second prism with a metaprism and maintain the geometry of the system (Figure 11, middle) we also obtain a parallel spectrum, but this time it does not leave the metaprism in the direction of the original beam.

Finally, Figure 11 (bottom) shows the combination of two N-SF11-M metaprisms. As in previous experiences, the angle of incidence has been inverted with respect to the normal, thus achieving a dispersion analogous to that of the first pair of prisms.

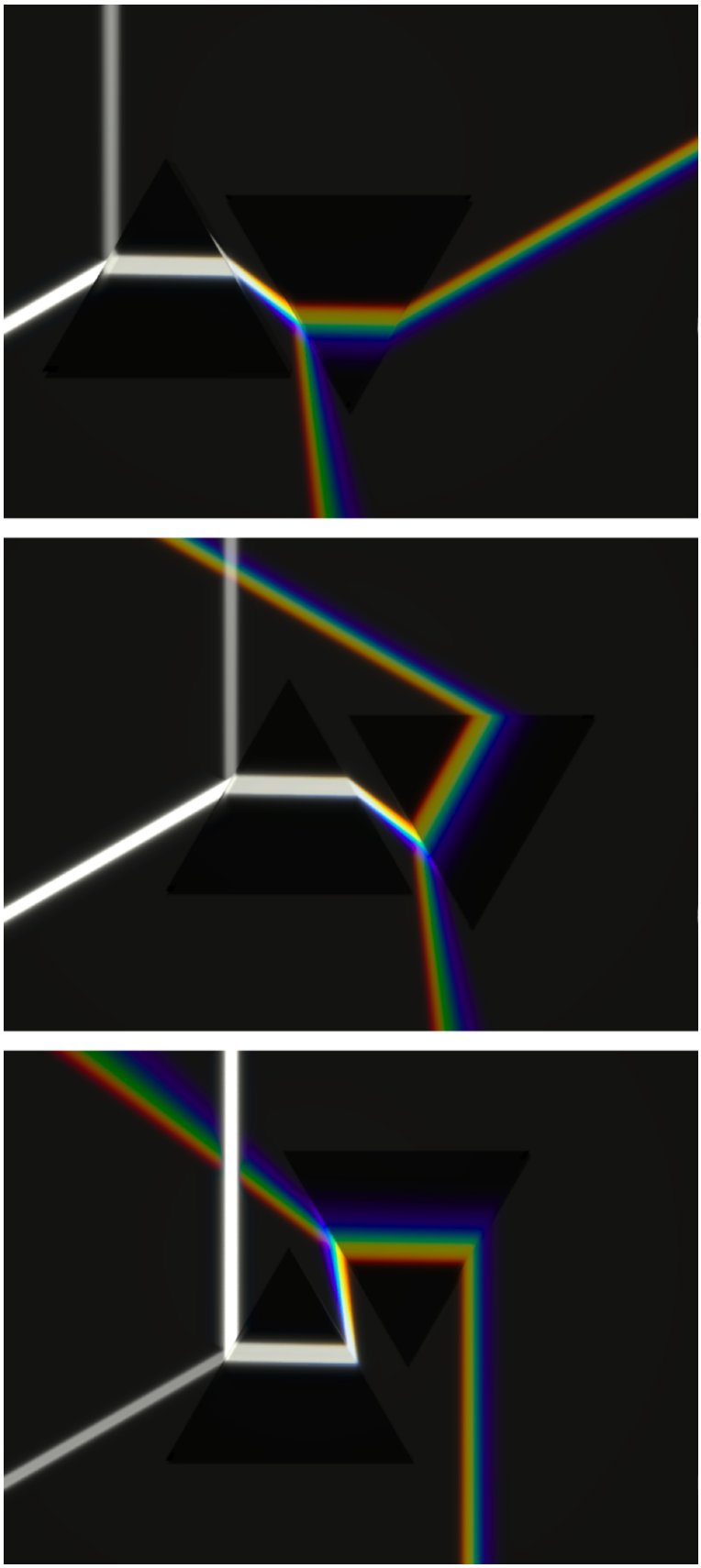

Figure 11. Different combinations of two elements: Prism-Prism (top); Prism-Metaprism (middle); Metaprism-Metaprism (bottom).

5. Conclusions

This study has successfully developed a valuable educational tool by presenting a collection of photorealistic images depicting prisms made with negative-index materials. These images serve as powerful visual aids that effectively illustrate the behavior of light in such prisms, contributing to a deeper understanding of their unique characteristics and spectral color dispersion phenomena. Generated using an open-source ray tracing program adapted for multispectral rendering, these images provide an immersive experience for students and educators alike.

Through a detailed comparison between the simulated metaprisms and their real counterparts, it has been observed that the refracted rays in negative-index prisms bend to the opposite side of the normal, resulting in a drastic change in the direction of the emerging beam. This comparison has also led to the establishment of a relationship between the deviation angles of conventional prisms and their corresponding metaprisms.

One notable finding of this study is that while the simulated metaprisms exhibit normal dispersion, the deviation angle significantly differs from that of normal prisms. Interestingly, it has been discovered that, under certain applications, the metaprisms can be utilized as real prisms if the angle of incidence is reversed. These intriguing results not only contribute to the understanding of negative-index materials but also raise important educational questions that stimulate further exploration and discussion.

The presented images not only provide a visual interpretation of the remarkable behavior of prisms made with negative-index materials but also offer a glimpse into how dispersion in metaprisms would appear in the visible domain. They allow educators to effectively demonstrate and explain the bending of light as it traverses negative-index prisms, leading to color dispersion. Moreover, the comparison between the behavior of light in conventional prisms and negative-index prisms, as depicted in the images, aids in elucidating the distinct properties and characteristics of negative-index materials.

Furthermore, the images generated in this study foster critical thinking and prompt students to delve deeper into the underlying principles and mechanisms of light propagation in negative-index prisms. By utilizing these images as visual aids, educators can enhance students' understanding of light behavior in both positive and negative index prisms, promoting active learning and facilitating the exploration of complex optical phenomena.

In summary, the presented images hold significant educational value, serving as a powerful tool for illustrating the behavior of prisms made with negative-index materials. They raise important questions, such as the need to reverse the angle of incidence and the absence of anomalous dispersion, thereby encouraging further exploration and facilitating meaningful discussions. The visual interpretation provided by these simulated images offers a captivating insight into the unique properties of negative-index materials and how spectral color dispersion manifests in metaprisms within the visible domain. Thus, these images are a valuable resource for high school students, pre-service science teachers, and

undergraduate students studying physics, providing a solid foundation for understanding and engaging with the fascinating world of optics.

References

[1] V. G. Veselago, 'The Electrodynamics of Substances with Simultaneously Negative Values of ε and μ', *Soviet Physics Uspekhi*, vol. 10, no. 4, pp. 509–514, Jan. 1968, doi: 10.1070/PU1968v010n04ABEH003699.

[2] R. A. Shelby, D. R. Smith, and S. Schultz, 'Experimental Verification of a Negative Index of Refraction', *Science (1979)*, vol. 292, no. 5514, pp. 77–79, Apr. 2001, doi: 10.1126/science.1058847.

[3] D. R. Smith, J. B. Pendry, and M. C. K. Wiltshire, 'Metamaterials and Negative Refractive Index', *Science (1979)*, vol. 305, no. 5685, pp. 788–792, Aug. 2004, doi: 10.1126/science.1096796.

[4] S. Linden, C. Enkrich, M. Wegener, J. Zhou, T. Koschny, and C. M. Soukoulis, 'Magnetic Response of Metamaterials at 100 Terahertz', *Science (1979)*, vol. 306, no. 5700, pp. 1351–1353, Nov. 2004, doi: 10.1126/science.1105371.

[5] C. Enkrich *et al.*, 'Focused-Ion-Beam Nanofabrication of Near-Infrared Magnetic Metamaterials', *Advanced Materials*, vol. 17, no. 21, pp. 2547–2549, Nov. 2005, doi: 10.1002/adma.200500804.

[6] S. Zhang, W. Fan, B. K. Minhas, A. Frauenglass, K. J. Malloy, and S. R. J. Brueck, 'Midinfrared Resonant Magnetic Nanostructures Exhibiting a Negative Permeability', *Phys Rev Lett*, vol. 94, no. 3, p. 37402, Jan. 2005, doi: 10.1103/PhysRevLett.94.037402.

[7] S. Zhang, W. Fan, N. C. Panoiu, K. J. Malloy, R. M. Osgood, and S. R. J. Brueck, 'Experimental Demonstration of Near-Infrared Negative-Index Metamaterials', *Phys Rev Lett*, vol. 95, no. 13, p. 137404, Sep. 2005, doi: 10.1103/PhysRevLett.95.137404.

[8] V. M. Shalaev *et al.*, 'Negative index of refraction in optical metamaterials', *Opt Lett*, vol. 30, no. 24, pp. 3356–3358, Dec. 2005, doi: 10.1364/OL.30.003356.

[9] A. N. Grigorenko *et al.*, 'Nanofabricated media with negative permeability at visible frequencies', *Nature*, vol. 438, pp. 335–338, Nov. 2005, doi: 10.1038/nature04242.

[10] J. Zhou, T. Koschny, M. Kafesaki, E. N. Economou, J. B. Pendry, and C. M. Soukoulis, 'Saturation of the magnetic response of split-ring resonators at optical frequencies', *Phys Rev Lett*, vol. 95, no. 22, p. 223902, Nov. 2005, doi: https://doi.org/10.1103/PhysRevLett.95.223902.

[11] M. W. Klein, C. Enkrich, M. Wegener, C. M. Soukoulis, and S. Linden, 'Single-slit split-ring resonators at optical frequencies: limits of size scaling', *Opt Lett*, vol. 31, no. 9, p. 1259, Jan. 2006, doi: 10.1364/OL.31.001259.

[12] G. Shvets and Y. A. Urzhumov, ‘Negative index meta-materials based on two-dimensional metallic structures’, *Journal of Optics A: Pure and Applied Optics*, vol. 8, no. 4, p. S122, Mar. 2006, doi: 10.1088/1464-4258/8/4/S11.

[13] C. Enkrich *et al.*, ‘Magnetic metamaterials at telecommunication and visible frequencies’, *Phys Rev Lett*, vol. 95, no. 20, p. 203901, Nov. 2005, doi: https://doi.org/10.1103/PhysRevLett.95.203901.

[14] A. Ishikawa, T. Tanaka, and S. Kawata, ‘Negative Magnetic Permeability in the Visible Light Region’, *Phys Rev Lett*, vol. 95, no. 23, p. 237401, Dec. 2005, doi: 10.1103/PhysRevLett.95.237401.

[15] A. Di Falco, M. Ploschner, and T. F. Krauss, ‘Flexible metamaterials at visible wavelengths’, *New J Phys*, vol. 12, no. 11, p. 113006, Nov. 2010, doi: 10.1088/1367-2630/12/11/113006.

[16] S. P. Burgos, R. de Waele, A. Polman, and H. A. Atwater, ‘A single-layer wide-angle negative-index metamaterial at visible frequencies’, *Nat Mater*, vol. 9, no. 5, pp. 407–412, Apr. 2010, doi: 10.1038/nmat2747.

[17] C. García-Meca, J. Hurtado, J. Martí, A. Martínez, W. Dickson, and A. V Zayats, ‘Low-loss multilayered metamaterial exhibiting a negative index of refraction at visible wavelengths’, *Phys Rev Lett*, vol. 106, no. 6, pp. 67402–67406, Feb. 2011, doi: 10.1103/PhysRevLett.106.067402.

[18] POV-Ray, ‘The Persistence of Vision Raytracer’, 2022. http://www.povray.org/

[19] G. Dolling, M. Wegener, S. Linden, and C. Hormann, ‘Photorealistic images of objects in effective negative-index materials’, *Opt Express*, vol. 14, no. 5, pp. 1842–1849, Mar. 2006, doi: 10.1364/OE.14.001842.

[20] J. Courtial and J. Nelson, ‘Ray-optical negative refraction and pseudoscopic imaging with Dove-prism arrays’, *New J Phys*, vol. 10, no. 2, p. 23028, Feb. 2008, doi: 10.1088/1367-2630/10/2/023028.

[21] A. J. Danner, ‘Visualizing invisibility: Metamaterials-based optical devices in natural environments’, *Opt Express*, vol. 18, no. 4, pp. 3332–3337, Feb. 2010, doi: 10.1364/OE.18.003332.

[22] F. L. Naranjo-Correa, G. Martínez-Borreguero, Á. L. Pérez-Rodríguez, P. J. Pardo-Fernández, and M. I. Suero-López, ‘Teaching rainbows with simulations: revisiting Minnaert’s lab experiment’, *Appl Opt*, vol. 56, no. 19, pp. G54–G69, May 2017, doi: 10.1364/AO.56.000G69.

[23] G. Martínez-Borreguero, F. L. Naranjo-Correa, Á. L. Pérez-Rodríguez, M. I. Suero-López, and P. J. Pardo-Fernández, ‘Comparative study of the effectiveness of three learning environments: Hyper-realistic virtual simulations, traditional schematic simulations and traditional laboratory’, *Physical Review Special Topics - Physics Education Research*, vol. 7, no. 2, p. 20111, Oct. 2011, doi: 10.1103/PhysRevSTPER.7.020111.

[24] G. Martínez-Borreguero, F. L. Naranjo-Correa, Á. L. Pérez-Rodríguez, M. I. Suero-López, and P. J. Pardo-Fernández, 'Use of computer generated hyper-realistic images on optics teaching: The case study of an optical system formed by two opposed parabolic mirrors', *Journal of Science Education*, vol. 14, no. 1, pp. 25–29, 2013.

[25] G. Martínez-Borreguero, F. L. Naranjo-Correa, Á. L. Pérez-Rodríguez, and M. I. Suero-López, 'Development of hyperrealistic simulations to teach concepts about colors', *Color Res Appl*, vol. 41, no. 3, pp. 330–332, Jun. 2016, doi: 10.1002/col.22013.

[26] D. D. Zhdanov, I. S. Potemin, V. A. Galaktionov, B. K. Barladyan, K. A. Vostryakov, and L. Z. Shapiro, 'Spectral ray tracing in problems of photorealistic imagery construction', *Programming and Computer Software*, vol. 37, no. 5, pp. 236–244, Sep. 2011, doi: 10.1134/S0361768811050069.

[27] R. I. Wahler, 'Spectral Rendering with POV-Ray', 2013. http://www.lilysoft.org/CGI/SR/Spectral Render.htm

[28] F. Kainz, R. Bogart, and P. Stanczyk, 'Technical introduction to OpenEXR', San Francisco, CA, Feb. 2009.

[29] J. W. Gooch, 'Encyclopedic Dictionary of Polymers', vol. 2. Springer, New York, pp. 653–654, 2011. doi: 10.1007/978-1-4419-6247-8_10447.

[30] M. N. Polyanskiy, 'Refractive index database', Mar. 2018. https://refractiveindex.info

[31] SCHOTT, 'Optical Glass - Data Sheets', Jul. 2017. [Online]. Available: https://schott.com/advanced_optics

[32] F. L. Naranjo-Correa and G. Martínez-Borreguero, 'Metaprisms Repository'. 2023. doi: https://doi.org/10.5281/zenodo.7997664.

[33] ISO and CIE, 'Joint ISO/CIE Standard: CIE Colorimetry – Part 2: Standard Illuminants for Colorimetry', San Francisco, CA, 2006.

Author's biographies

Francisco L. Naranjo-Correa is a Lecturer in the Faculty of Education and Psychology at the University of Extremadura (UEx). Previously, he worked for 15 years as a Research Project Manager in the field of Physics and Mathematics.

He holds a Bachelor's degree in Physics, a Master's degree in Optics and Physics Education, and obtained his Doctorate in Physics with a thesis entitled "Light and Color: Development of didactic tools to enhance their teaching in pre-service teachers."

Throughout his career, he has participated in various research projects focused on the didactics of experimental sciences, STEM education, the detection of misconceptions, concept maps, and collaborative learning. He has also been involved in several educational innovation projects, applying innovative pedagogical approaches in science education, and is a member of the research group "Professional Development of Science and Mathematics Teachers."

He has published over 20 papers in prestigious indexed journals and contributed to several book chapters. Additionally, he has participated in nearly 100 national and international conferences, where he has shared his research and knowledge with the academic community.

His research interests span various fields, including science education, pedagogical content knowledge, photorealistic simulations, and the development of multimedia didactic tools.

Guadalupe Martínez-Borreguero is a Senior Lecturer at the Department of Science Education at the University of Extremadura (UEx) and a member of the Institute for Educational Research and Prospecting (INPEX).

She holds a Bachelor's degree in Physics and a Bachelor's degree in Materials Engineering, receiving extraordinary honors in both disciplines. She also holds a Master of Science specializing in Physics Education and a University Specialist degree in Information and Communication Technologies applied to university teaching. She completed her doctorate in the field of Physics Education and is a member of the research group "Professional Development of Science and Mathematics Teachers."

In her research group, she has sought to integrate research and teaching in a dedicated line of research focused on science education. She has participated in various research projects related to science education and has led a project on STEM education at different educational levels.

She has been a speaker at numerous national and international conferences and has published in prestigious international and national journals, with over 40 papers indexed in reputable databases. Her research interests encompass the teaching and learning of STEM areas from the perspective of affective and cognitive domains, education for sustainable development, and the development of didactic materials. She has authored

over 50 book chapters and made more than 200 scientific contributions to conferences, mostly as oral presentations, all related to the research field of Science Education.

Her research interests include teaching and learning of STEM areas, affective and cognitive domains, education for sustainable development and development of didactic materials.